Contig Maps and Genomic Sequencing Identify Candidate Genes in the Usher 1C Locus

Michael J. Higgins, Colleen D. Day, Nancy J. Smilinich, et al.

Genome Res. 1998 8: 57-68
Access the most recent version at doi:10.1101/gr.8.1.57

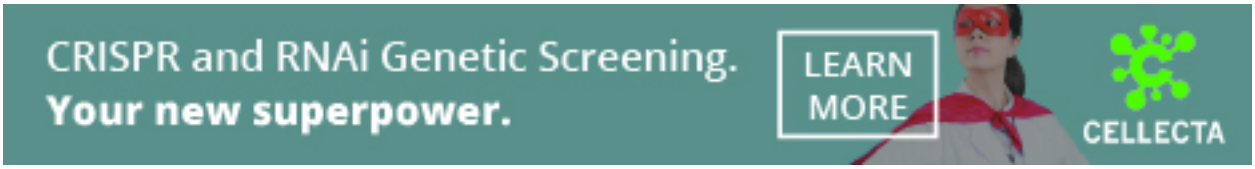

LETTER

Contig Maps and Genomic Sequencing Identify Candidate Genes in the Usher 1C Locus

Michael J. Higgins,[1,6] Colleen D. Day,[1] Nancy J. Smilinich,[1] L. Ni,[2] Paul R. Cooper,[1] Norma J. Nowak,[1] Chris Davies,[4,5] Pieter J. de Jong,[1] Fielding Hejtmancik,[3] Glen A. Evans,[4] Richard J.H. Smith,[2] and Thomas B. Shows[1]

[1]Department of Human Genetics, Roswell Park Cancer Institute, Buffalo, New York 14263 USA, [2]Department of Otolaryngology, University of Iowa, Iowa City, Iowa 52242 USA; [3]National Eye Institute, National Institutes of Health, Bethesda, Maryland 20892 USA; [4]The McDermott Center for Genome Research, University of Texas Southwestern Medical Center, Dallas, Texas 75235 USA

Usher syndrome 1C (USH1C) is a congenital condition manifesting profound hearing loss, the absence of vestibular function, and eventual retinal degeneration. The USH1C locus has been mapped genetically to a 2- to 3-cM interval in 11p14–15.1 between *D11S899* and *D11S861*. In an effort to identify the USH1C disease gene we have isolated the region between these markers in yeast artificial chromosomes (YACs) using a combination of STS content mapping and *Alu*–PCR hybridization. The YAC contig is ~3.5 Mb and has located several other loci within this interval, resulting in the order *CEN-LDHA-SAA1-TPH-D11S1310-(D11S1888/KCNC1)-MYOD1-D11S902-D11S921-D11S1890-TEL*. Subsequent haplotyping and homozygosity analysis refined the location of the disease gene to a 400-kb interval between *D11S902* and *D11S1890* with all affected individuals being homozygous for the internal marker *D11S921*. To facilitate gene identification, the critical region has been converted into P1 artificial chromosome (PAC) clones using sequence-tagged sites (STSs) mapped to the YAC contig, *Alu*–PCR products generated from the YACs, and PAC end probes. A contig of >50 PAC clones has been assembled between *D11S1310* and *D11S1890*, confirming the order of markers used in haplotyping. Three PAC clones representing nearly two-thirds of the USH1C critical region have been sequenced. PowerBLAST analysis identified six clusters of expressed sequence tags (ESTs), two known genes (*BIR,SUR1*) mapped previously to this region, and a previously characterized but unmapped gene *NEFA* (DNA binding/EF hand/acidic amino-acid-rich). GRAIL analysis identified 11 CpG islands and 73 exons of excellent quality. These data allowed the construction of a transcription map for the USH1C critical region, consisting of three known genes and six or more novel transcripts. Based on their map location, these loci represent candidate disease loci for USH1C. The NEFA gene was assessed as the *USH1C* locus by the sequencing of an amplified *NEFA* cDNA from an USH1C patient; however, no mutations were detected.

[The sequence data described in this paper have been submitted to GenBank under accession numbers AC000406–AC000407.]

Usher (USH) syndrome refers to a heterogeneous collection of disorders characterized by congenital hearing impairment, retinitis pigmentosa, and variable vestibular dysfunction. USH syndrome has been divided into three clinical types (Kimberling and Moller 1995): Patients with type I disease (USH1) have severe congenital hearing loss and the absence of vestibular function; in type II disease (USH2) the hearing loss is congenital but moderate to severe and there is no disruption of vestibular capacity; patients with type III disease (USH3) are distinguished from USH2 patients by a progressive loss of hearing. Progressive pigmentary retinopathy is a feature of all three types of USH syndrome.

The complex clinical picture is reflected in the genetic heterogeneity of the disease. At least eight different loci have been identified that contribute to these autosomal recessive disorders. The majority of

[5]Present address: Bayer Corporation, Berkeley, California 94701 USA.
[6]Corresponding author.
E-MAIL higgins@shows.med.buffalo.edu; FAX (716) 845-8449.

USH2 families exhibit genetic linkage to markers on the long arm of chromosome 1 (USH2A; Kimberling et al. 1990; Kimberling and Moller 1995), whereas the disease locus in one large family segregating USH2 does not (Pieke-Dahl et al. 1993). The *USH3* locus has been assigned to the long arm of chromosome 3 at 3q21–25 (Sankila et al. 1995). At least five loci are implicated in the development of type I disease. *USH1A* has been mapped to 14q32 (Kaplan et al. 1992), whereas the *USH1B* and *USH1C* genes have been localized to the long and short arms, respectively, of chromosome 11 (Kimberling et al. 1992; Smith et al. 1992). More recently, two additional USH1 loci have been identified, *USH1D* at chromosome 10q (Wayne et al. 1996) and *USH1E*, which maps to chromosome 21q21 (Chaib et al. 1997).

The locus responsible for USH1B (11q13) has been identified as an unconventional myosin VIIA gene (Weil et al. 1995), a finding consistent with the observation that USH syndrome patients exhibit a generalized disorganization of microtubules in the axoneme of sensory hair cells. This gene also appears to be involved in certain cases of hereditary nonsyndromic deafness (DFNB2; Liu et al. 1997; Weil et al. 1997). Whether mutations in genes encoding additional unconventional myosins or proteins that interact with them result in other types of USH syndrome awaits the isolation of the remaining disease loci.

The location of the *USH1C* locus was initially assigned to 11p14–15.1 (Smith et al. 1992) and was later refined by linkage and haplotype analysis to the 2- to 3-cM interval between *D11S889* and *D11S861* (Keats et al. 1994). To identify the gene responsible for *USH1C* we undertook the isolation of the critical region in yeast artificial chromosomes (YACs). Haplotyping of affected patients with additional markers ordered by somatic cell hybrids and the YAC contig narrowed the *USH1C* locus to between *D11S902* and *D11S1890*. To facilitate subsequent transcript identification, the interval between *D11S1310* and *D11S1890* has been converted to PACs. Large-scale sequencing of a portion of this contig has resulted in the identification of several transcripts within the USH1C critical region. These transcripts are being tested as candidates for the *USH1C* locus.

RESULTS

Generation of a YAC Map through the USH1C Region

The location of Usher syndrome 1C (*USH1C*) was originally determined to be in the interval flanked by *D11S861* and *D11S889* on chromosome 11p14–15.1 (Keats et al. 1994). A number of markers believed to map near or within this region (James et al. 1994; Keats et al. 1994; Fantes et al. 1995) were ordered in a panel of somatic cell hybrids (data not shown) as indicated in Figure 1A. Following PCR screening of a chromosome 11 YAC library (Qin et al. 1993), small contigs were assembled around markers for the genes *LDHA*, *SAA1*, *TPH*, *KCNC1*, and *MYOD1*, as well as microsatellites *D11S419*, *D11S1310*, *D11S902*, *D11S921*, *D11S1888*, and *D11S1890* (Fig. 1B). The contigs were verified by Southern analysis using STSs and single copy gene markers as hybridization probes. Overlap detected by hybridization of *Alu*–PCR products was confirmed by Southern analysis of *Alu*–PCR fingerprints (Qin et al. 1996). Finally, YACs representing the shortest path through each contig were mapped to 11p14–15.1 by FISH (see Fig. 1B).

In an effort to join these contigs, the CEPH mega-YAC library was screened for *D11S1310*, resulting in a single positive clone (804C12). *Alu*–PCR products generated from this CEPH mega-YAC were then hybridized to pooled *Alu*–PCR products of the chromosome 11-specific YAC library (Qin et al. 1996) identifying each of the smaller YAC contigs except those containing *D11S419* and *D11S1890*. End probes were derived from two *D11S1890*–YACs by a ligation-mediated PCR method (Kere et al. 1992) and found to hybridize to the single *D11S921*-containing YAC, yRP-2f11. Closure of the gap between the *D11S419*–contig and the larger contig was not attempted, as *D11S419* mapped outside the critical region defined by reconstruction of haplotypes (see below).

The STS/probe content of each YAC, along with clone size, was analyzed by the contig assembly program SEGMAP (Green and Green 1991). This algorithm generated a clone contig consisting of >40 YACs from *LDHA* proximally to beyond (distal) *D11S1890* encompassing ~3.5 mb. The contig contains markers for five genes, five microsatellites, two anonymous STSs (*D11S1168*, *D11S1122*), four YAC ends, and 34 *Alu*–PCR products. The predicted order is *CEN-LDHA-SAA1-D11S1168-TPH-D11S1310-D11S1122-(D11S1888/KCNC1)-MYOD1-D11S902-D11S921-D11S1890-TEL*.

Reconstruction of USH1C Haplotypes

Using microsatellite markers ordered by the contig, haplotype analysis was carried out on USH1C family members which narrowed the critical disease locus region to between *D11S902* and *D11S1890* (Table

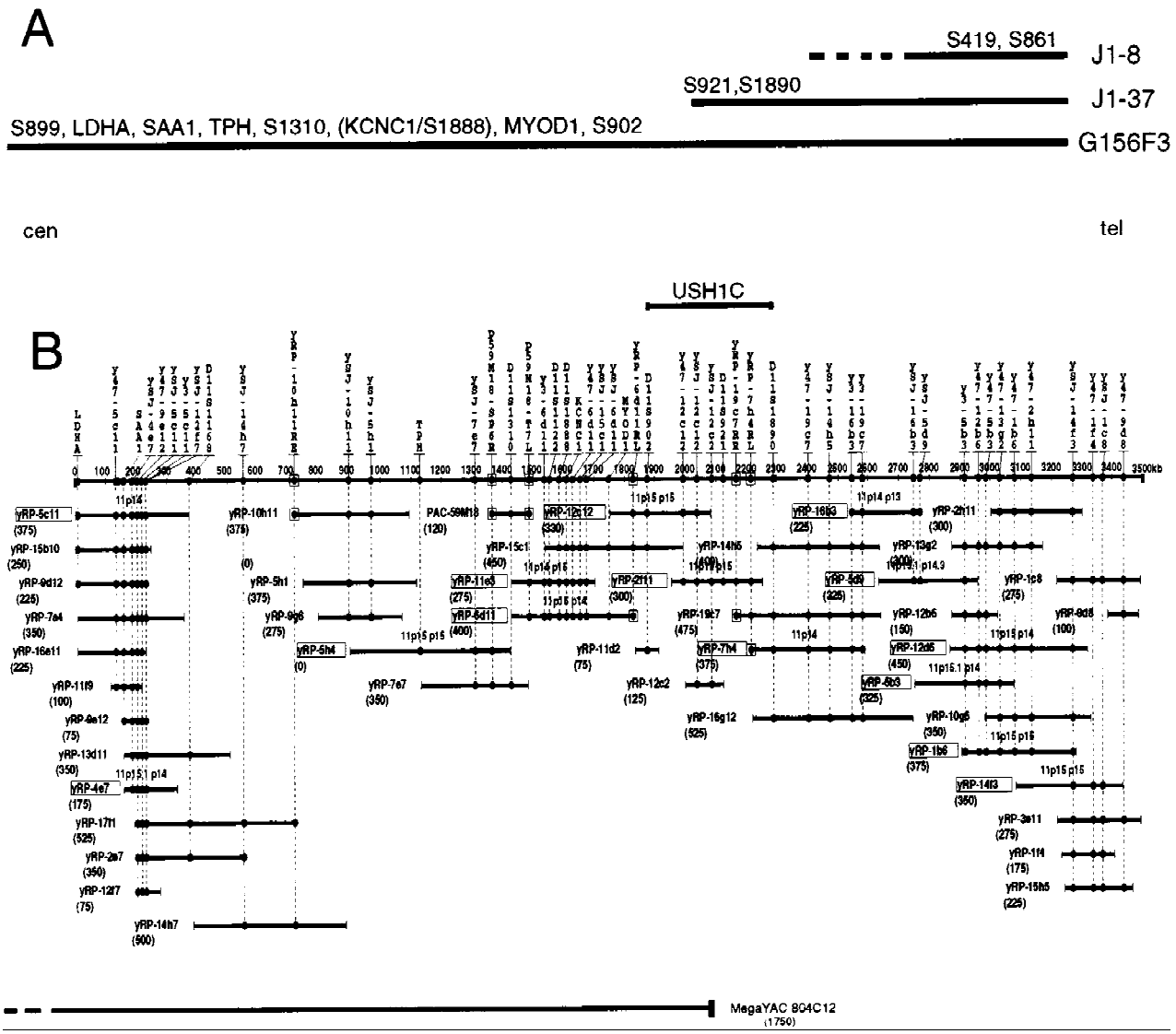

Figure 1 Physical maps of the USH1C region. (*A*) Somatic cell hybrids were used initially to bin markers believed to map between *D11S889* and *D11S861.* The heavy lines represent the approximate extent of chromosome 11 from pter contained in each hybrid cell line. The order within each bin is based on the YAC map below. The placement of markers *D11S899, D11S419,* and *D11S861* on the hybrid panel was determined by Fantes et al. (1995). These markers are for reference only and are not present within the clone contig. (*B*) YAC contig of USH1C critical and flanking regions. The contig was assembled by SEGMAP using both STS content and *Alu*–PCR hybridization data. YAC names and sizes (kb) are shown to the *left* of each clone and in parenthesis, respectively. For some clones (boxed), the cytogenetic position determined by FISH is indicated above the horizontal line representing the YAC. Markers contained within the contig are shown above the contiguous line that represents the genomic map. Markers with the prefix y47, y3, or ySJ are *Alu*–PCR probes generated from the named YAC clone using one of three *Alu* primers as described (Qin et al. 1996). Marker names prefixed with yRP and ending with RR, ER, or RL are end probes generated from the named YAC clone. The only link between the *LDHA/SAA1*-containing clones and the remainder of the contig is through the mega-YAC 804C12 determined by *Alu*–PCR hybridization. The proximity of these clones with the rest of the contig is consistent with other YAC contigs in this region (Sellar et al. 1994; Ayyagari et al. 1996). The ends of a PAC clone (59M18) were used to show a second link between the *TPH* YAC clones and *KCNC1/S1888/MYOD1* YAC clones.

1). Based on the YAC contig assembled by SEGMAP, the USH1C critical region is ~400 kb (Fig. 1B). Because all affected individuals, and no carrier or unaffected person from the Acadian population tested,

Table 1. USH1C Haplotypes

Patient	CEN–1310	1888	902	921	1890–TEL
Consensus haplotype (n = 13)	1, 1	1, 1	4, 4	3, 3	2, 2
2	1, 2	1, 1	4, 7	3, 3	2, 2
10	1, 3	1, 1	4, 4	3, 3	2, 2
11	2, 3	1, 1	4, 4	3, 3	2, 2
15	3, 3	2, 3	4, 7	3, 3	1, 2
28	1, 2	1, 3	4, 4	3, 3	2, 2

No carrier or nonaffected individual from the Acadian area who has been screened is homozygous for 921.

were homozygous for allele 3 at *D11S921* (Table 1), the disease gene is likely to be located in the middle of the contig close to this marker.

PAC Contig of USH1C Critical Region

To facilitate the identification of transcribed sequences in the USH1C critical region, part of the YAC contig was ''converted'' to large-insert bacterial clones using a PAC library (Ioannou et al. 1994). Initially, *Alu*–PCR products generated from several YAC clones were pooled and hybridized to high-density PAC filters. After secondary screening with *Alu*–PCR products from individual YACs, the clones were characterized by pulsed-field gel electrophoresis, STS analysis with microsatellite and gene markers, and Southern hybridization to the original YAC contig. To complete the contig, end probes were rescued from selected PAC clones (Cooper et al. 1997) and used to rescreen the PAC library by hybridization. End probes were also used to verify overlap between adjacent clones by Southern analysis. As they became available, expanded portions of the PAC library were screened by hybridization using microsatellite and PAC end probes to increase contig depth. To help verify the contig, 15 PACs representing the shortest path between *D11S1310* and *D11S1890* were mapped to 11p14–15.1 by FISH (Fig. 2).

Analysis by SEGMAP generated a 1.3-mb contig consisting of 55 clones and 42 markers including 5 microsatellite markers and 31 PAC end probes. The sulfonylurea receptor 1 (*SUR1*) gene, a candidate disease gene for familial persistent hyperinsulinemic hypoglycemia (PHHI; Thomas et al. 1995) and the β-cell inward rectifying potassium channel (*BIR*) gene, both of which had been mapped previously to this region (Ayyagari et al. 1996), were positioned in the contig and ordered with respect to other markers. Sequence analysis of a CpG island shared by PACs 169P3 and 306B4 identified a 5′ exon from the previously unmapped *NEFA* protein gene (Barnikol-Watanabe et al. 1994). PCR and Southern analysis located *NEFA* just centromeric to *D11S921* (Fig. 2). The higher resolution of the PAC map (cf. YAC contig) permitted the placement of *D11S1888* telomeric to *KCNC1* (Fig. 2). Finally, the order of markers defined by this contig is *CEN-D11S130-KCNC1-D11S1888-MYOD1-D11S902-SUR1-BIR-NEFA-D11S921-D11S1890-TEL*, confirming and refining the order defined by the YAC contig (Fig. 1B).

Large-Scale Sequencing through the USH1C Critical Region

The combination of large-scale genomic sequencing and the availability of the unprecedented resource of dbEST (and the corresponding cDNA clones) has allowed us to greatly increase the density of potential candidate genes in the USH1C region. Three PAC clones (239B22, 306B4, and 169P3) have been sequenced thus far, providing close to 300 kb of sequence in 10 contigs (Table 2; GenBank accession nos. AC000406–AC000407). The sequence data were analyzed with PowerBLAST (Zhang and Madden 1997), a newly developed program that provides graphic representations of BLAST searches, and the exon-prediction algorithm GRAIL.

Known Genes

Table 2 summarizes the PowerBLAST results obtained to date. Not surprisingly, the *SUR1* gene and the *BIR* gene were identified in the available sequence (Fig. 3). The *SUR1* gene is large, consisting of

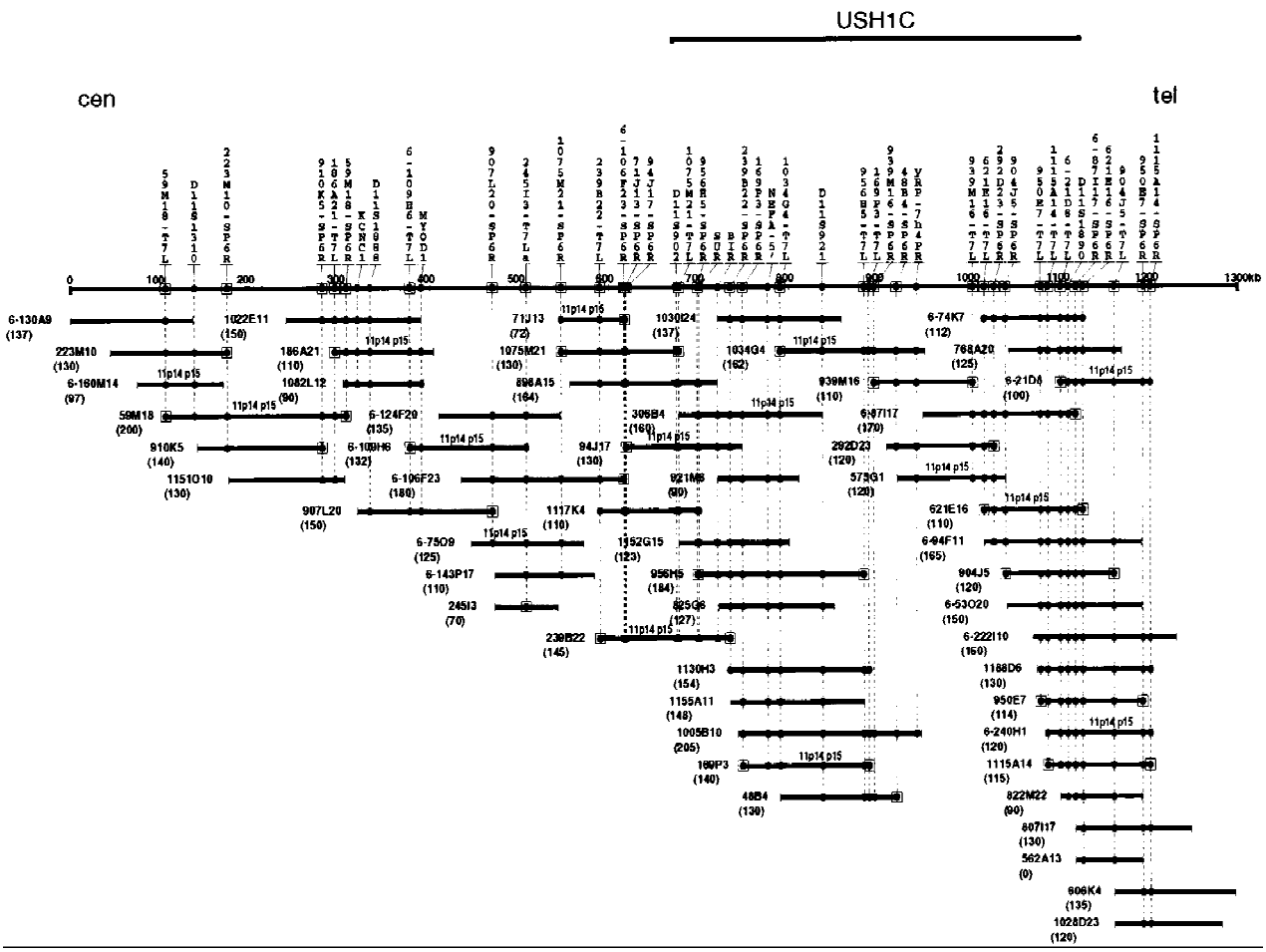

Figure 2 PAC clone contig of the USH1C region generated by SEGMAP using STS content mapping and YAC-derived *Alu*–PCR and PAC end probe hybridization data. Clone names and sizes (kb) are indicated as in Fig. 1B. Marker names ending with SP6R or T7L are PAC end probes generated from the SP6 and T7 ends, respectively, of the indicated clone.

39 exons (Nestorowicz et al. 1996) and spread over at least 100 kb. The *BIR* gene appears to be intronless and is linked closely to *SUR1* in a head-to-tail orientation with both genes being transcribed in the centromeric to telomeric direction (Fig. 3). PowerBLAST analysis of sequence contigs 771, 773, and 774 identified the *NEFA* gene. Comparison of the cDNA with the genomic sequence allowed us to generate a complete gene map of *NEFA* with 12 exons distributed over at least 60 kb.

Expressed Sequence Tags / Novel Genes

PowerBLAST analysis against dbEST showed six hits in five sequence contigs, all but one of which had 90%–99% homology (Table 2). Further alignment of these ESTs to the genomic sequence indicated that at least two appear to represent more than one exon, a finding supporting the notion that these ESTs represent true genes rather than pseudogenes. None of these ESTs showed significant homology to any known genes. Interestingly, EST cluster 5 (ESTc5) maps to an intron in the NEFA gene (Fig. 3). Because this EST appears to be transcribed in the same direction as NEFA, it is possible that it may represent unidentified exons of this gene, although this seems unlikely considering that the vast majority of EST cDNAs were primed with oligo(dT) at their 3′ ends. Two separate EST clusters (ESTc2 and ESTc3) were found 20 kb downstream of the BIR gene (Fig. 3). These EST clusters both show more than one exon, and are in divergent orientation with one within an intron of the other. One of these potential genes (ESTc2) was also detected in the retina at the level of RT–PCR (not shown).

Table 2. Transcripts Identified by Sequencing the USH1C Critical Region

Contig (kb[a])	PAC	Known genes	STSs[b]	ESTc (%ID/length) (rep. clone)[c]	GRAIL exons[d]	CpG islands[e]
761 (7)	169p3					
765 (9)	169p3	*RP-S4/S25* pseudogenes[f]	SHGC3156		5	2
766 (13)	239b22	*SUR1*[g]			5	
767 (13)	169p3				2	
770 (25)	169p3		*D11S1228*			
771 (18)	169p3/306b4	*NEFA*[h]		6 (80/185)(R63988)		1
773 (23)	169p3/306b4	*NEFA*[h]	AFMb340wf5	5 (99/618)(R02788)	3	1
774 (38)	169p3/306b4	*NEFA*[h]		4 (96/63)(AA091720)	10	1
775 (50)	239b2	*SUR1*[g]		1 (97/480)(H09680)	18	2
776 (85)	306b4/239b22	*SUR1*[g], *BIR*[i]		2 (98/460)(H73741) 3 (99/534)(W93954)	29	4
Total sequenced 281						

[a]Number of kilobase pairs in sequence contig. Genomic sequence data are available using GenBANK accession nos. AC000406 and AC000407.
[b]Sequenced-tagged sites.
[c]Expressed sequenced-tagged site cluster. (%ID/length) percent identity/length of homologous region, GenBank accession no. for representative clone.
[d]Number of GRAIL-predicted exons of ''excellent'' quality.
[e]CpG islands as defined by Gardiner-Garden and Frommer (1987).
[f]Pseudogenes for ribosomal proteins S4 and S25.
[g](*SUR1*) Sulfonylurea receptor 1 (GenBank accession nos. L78207–L78243).
[h](*NEFA*) DNA binding/ EF-hand/acidic-amino acid rich protein (GenBank accession no. X76732).
[i](*BIR*) β-Cell inward rectifier potassium channel gene (GenBank accession no. D50582).

Exon and CpG Island Prediction Using GRAIL

The 281 kb of sequence through the USH1C critical region was also analyzed by the exon prediction program GRAIL using the ORNL web page (see Methods). The results are summarized in Table 2 as are predictions of CpG islands (likely locations of genes) determined on the same website, as defined by Gardiner-Garden and Frommer (1987). Seventy-three exons of excellent quality (most likely to be bona fide exons) were predicted. A large number of ''good'' quality exons were also identified, some of which may also be true exons. Many of these, but not all, were found to be exons of *SUR1* and *NEFA* or to colocalize with DNA segments homologous with ESTs identified with PowerBLAST.

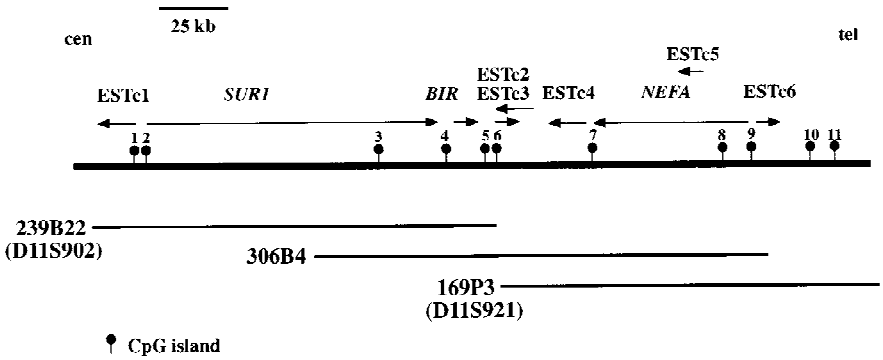

Figure 3 Transcript map of a portion of the USH1C critical region. Known genes and ESTs are shown relative to the sequenced PAC clones. Arrows indicate the direction of transcription; CpG islands are indicated as lollipops.

Eleven CpG islands were identified in the available sequence. Some of these were found to be near or within the first exon of known genes (e.g., *BIR*, *SUR1*, *NEFA;* Fig. 3). Other CpG islands were associated with ESTs or with 10 exons of ''excellent'' quality that do not appear to be associated with any of the known genes or ESTs (e.g., CpG islands 10 and 11 in sequence contig 765). These 10 exons may, therefore, represent portions of additional novel genes in the region.

Mutation Analysis of *NEFA* in USH1C Patient cDNA

The predicted amino acid sequence of *NEFA* indicates the presence of a DNA-binding domain containing a leucine zipper and two helix–loop–helix (HLH) domains that exhibit EF hand motifs, a property of certain Ca^{2+}-binding proteins. Barnikol-Watanabe et al. (1994) postulate that these sites may play a role in the modification of protein folding similar to that seen for calmodulin (Strynadka and James 1989). The presence of EF hand domains in *NEFA* protein suggested the possibility that this protein could interact with unconventional myosins in a manner analogous to calmodulin (Wolenski 1995). If true, *NEFA* would be an attractive candidate gene considering that the *USH1B* locus encodes unconventional myosin VIIA (Weil et al. 1995).

Because a founder effect is likely for USHIC in the Acadian families segregating the disease (Smith et al. 1992), only one mutant allele is expected to be present in this population. For this reason, we opted to do mutation analysis by sequencing to approach 100% detection efficiency. Primers were designed to amplify the 1.6-kb *NEFA* cDNA in four overlapping amplimers of ~450 bp each. Following PCR, the products were sequenced in both directions. No changes in the nucleotide sequence of the amplified *NEFA* cDNA were observed in USH1C patients compared to normal.

DISCUSSION

The *USH1C* locus was originally mapped in French–Acadian families by linkage and haplotype analysis between *D11S861* and *D11S899* (Keats et al. 1994). Toward the positional cloning of the USH1C disease gene, we have constructed a 3.5-Mb YAC contig encompassing loci mapping between these flanking markers (Weissenbach et al. 1992; James et al. 1994; Keats et al. 1994; Fantes et al. 1995). Although this region has been isolated previously using CEPH mega-YACs, the order of many critical markers could not be established definitely because of apparent deletions or other rearrangements in the YAC clones (Ayyagari et al. 1996). Furthermore, many of the YACs were chimeric, limiting their downstream utility (Ayyagari et al. 1996). Except for a single mega-YAC, the contig presented here consists of smaller chromosome 11-specific YACs, which have a lower incidence of rearrangement and chimerism (Qin et al. 1993, 1996). Many of the previously unordered markers in earlier mega-YAC contigs (Chumakov et al. 1995; Ayyagari et al. 1996) were ordered in the present clone contig (Fig. 1B). This order was consistent with that determined by the single-linked mega-YAC contig but not the double-link contig constructed by The Whitehead Institute/MIT Center for Genome Research (1997). Our marker order is also at odds with the placement of *D11S921* and *D11S1890* centromeric to *D11S902* and *D11S1888* by radiation hybrid mapping; however, the latter order was not established at 1000:1 odds (James et al. 1994). The order determined in the YAC contig shown in Figure 1B is consistent with that determined by somatic cell hybrid mapping, although it could be argued that these two methods are not independent, as both the hybrid mapping panel and the chromosome 11 YAC library were derived from the monochromosomal hybrid J1 (Koa et al. 1976; Qin et al. 1993). However, the order was confirmed by STS-content mapping using PAC clones (Fig. 2) that were made from an independent DNA source (Ioannou et al. 1994).

The confirmed order of microsatellite markers (*CEN-S1310-S1888-S902-S921-1890-TEL*) allowed reconstruction of haplotypes of affected individuals that pointed to the 400-kb region between *D11S902* and *D11S1890* (Fig. 1B; Table 1) as harboring a gene involved in USH1C. This localization represents a significant (five- to eightfold) reduction in the size of the critical region for this disease. Based on earlier mapping studies (Ayyagari et al. 1996), the genes coding for the potassium channel protein *KCNC1* and myogenic factor 3 (*MYOD1*) were considered as candidate loci for USH1C. Our refinement of the critical region to between D11S902 and *D11S1890* now excludes these two loci as the disease-associated gene (Figs. 1B and 2), consistent with failure to detect mutations in the *KCNC1* gene in USH1C patients (Marietta et al. 1997).

The *tubby* and *rd5* mouse phenotypes display both retinal and cochlear degeneration and have been suggested as murine models for Usher syndrome, as these mutations map to distal mouse chromosome 7, which is partially syntenic to 11p15 (Heckenlively et al. 1995; Ohlemiller et al. 1995; Chung et al. 1996). However, based on both genetic and physical mapping studies, a relationship with USH1C seems unlikely. Chung et al. (1996) mapped the mouse *tub* locus near *Hbb* >14 cM distal to *Sur*, the human homolog of which maps within the USH1C critical (this study; Ayyagari et al. 1996). Kleyn et al. (1996) identified *tub* exons in a mouse P1 clone that also contained the *Rbtn1* gene. In humans, pulsed-field gel electrophoresis locates *RBTN1* >6 mb telomeric to *MYOD1* (Higgins et al. 1994), which maps very close to the *USH1C* locus (Figs. 1 and 2). Thus, *USH1C* and *tub* appear to be

distinct genetic loci. Similarly, the *Rd5* mouse is unlikely to be the murine homolog of USH1C, as the *Rd5* locus maps only 2 cM from *Hbb* (Hechenlively et al. 1995). The human *STEP* (striatum-enriched phosphatase) gene was mapped to 11p15.1–15.2 and was suggested as a potential candidate for USH1C (Li et al. 1995). PCR analysis of the PAC contig shown in Figure 2 with primers for *STEP* was negative indicating that this gene does not map within the USH1C critical region.

Mutations in genes coding for unconventional myosins result in USH1B (Weil et al. 1995), DFNB2 (Liu et al. 1997; Weil et al. 1997), and the mouse *Snell's waltzer* mutant (Avraham et al. 1995). To determine whether a similar situation exists in USH1C, the shortest path of PACs through the critical region was hybridized at normal and reduced stringency (2× SSC, 0.5% SDS at 55°C) with a cDNA clone corresponding to the unconventional myosin VIIA gene (USH1B locus). Consistent with a similar experiment (Ayyagari et al. 1996), no specific hybridization was observed (not shown).

The PAC contig has provided reliable DNA templates for large-scale genomic sequencing. PowerBLAST and GRAIL analyses of the available sequence have allowed the construction of a transcript map encompassing roughly two-thirds of the USH1C critical region. This map permitted the precise localization and transcriptional orientation of two genes (*BIR, SUR1*) that had been shown previously to map to this region (Ayyagari et al. 1996) as well as the unmapped, but previously described gene *NEFA* (Barnikol-Watanabe et al. 1994). Large-scale sequencing and computational analyses also identified a collection of potential novel genes in the USH1C critical region as evidenced by clusters of ESTs, CpG islands, and GRAIL-predicted exons (Table 2; Fig. 3). Because of their localization, these genes and novel transcripts represent candidate disease genes for USH1C.

By Northern blot, *SUR1* and *BIR* are primarily expressed in the islet cells of the pancreas (Inagaki et al. 1995), although we have detected low-level expression of these two genes in retina by RT-PCR (not shown), making them candidate genes for USH1C. However, loss-of-function mutations in the *SUR1* gene have been identified in some patients with PHHI (Thomas et al. 1995), a condition typified by unregulated secretion of insulin. Given the precedents of other syndromic and nonsyndromic forms of hearing loss [e.g., MYOVIIA in USH1B (Weil et al. 1995), PAX3 in Waardenburg syndrome (Baldwin et al. 1992; Tassabehji et al. 1992), and Cx26 in DFNB1 (Kelsell et al. 1997)], it is likely that alterations in the *USH1C* gene will also be loss-of-function mutations. There is no apparent phenotypic overlap between PHHI and USH1C, making it unlikely that the *SUR1* gene is involved in USH. It has been suggested that the *BIR* protein may interact with the *SUR1* gene product in the formation of one or more pancreatic β-cell potassium channels (Inagaki et al. 1995). If true, then the lack of characteristics in common between PHHI and USH1C patients also argues against *BIR* being the locus responsible for USH1C.

The *NEFA* gene maps to a PAC clone that also contains D11S921, a marker found to be homozygous for allele 3 in all patients affected with *USH1C* (Fig. 3; Table 2). Its map location as well as some speculative properties of the NEFA protein, prompted us to test this gene for mutations in patients. However, sequence analysis of the *NEFA* cDNA of a USH1C patient failed to reveal any mutation in the protein coding region. This result, however, does not exclude the involvement of *NEFA* and USH1C, as mutations affecting regulatory regions have not been assessed. Further assessment of this gene as a candidate for USH1C is warranted.

As indicated in Table 2, PowerBLAST analysis identified the microsatellite markers AFMb340wf5 within the *NEFA* gene. A computer search of the available genomic sequence identified four additional loci with sufficient dinucleotide repeats to be polymorphic. Additional haplotyping of USH1C patients with these markers should prove useful in further narrowing the critical region.

The PAC clone contig presented here should greatly facilitate the identification of the gene associated with USH1C. The ease (cf. YACs) in obtaining high-quality DNA from clones representing the USH1C critical region has resulted in the identification of several ESTs or potential candidate genes by large-scale sequencing and computer analysis. These same reagents can be used for complementary gene finding approaches, such as exon trapping and cDNA selection. The identification and characterization of the USH1C disease gene and its product will aid in our understanding of both syndromic and nonsyndromic hereditary hearing loss in general and in the pathology of USH syndrome in particular.

METHODS

Patient Identification

Individuals with the presumed diagnosis of USH1 were examined at the Catholic Deaf Center (LaFayette, LA). The diagno-

sis of USH1 was established by clinical criteria (Smith et al. 1994). French–Acadian USH1C families investigated in this study are described in Smith et al. (1992).

Genotyping

To determine individual genotypes, 30 ml of blood was collected from each person in EDTA-containing tubes. Genomic DNA was prepared from peripheral lymphocytes (Grimberg et al. 1989) and amplified by PCR as described previously (Smith et al. 1992). Markers selected for analysis were known to be tightly linked to the USH1C locus (this study; Smith et al. 1992; Keats et al. 1994).

Hybrid Panel Analysis

Genomic DNAs (100 ng) from J1-4b, J1-8, J1-37 (Koa et al. 1976), NW (Gessler et al. 1989), human (GM00131), and hamster (CHW1102) were tested by PCR for the presence of *D11S416, D11S902, D11S921, D11S1310, D11S1888,* and *D11S1890*. Primer pairs were obtained from GDB. *MYOD1,* and *KCNC1,* were mapped by Southern hybridization using the same DNA and plasmid probes Myf3 and HNGK4, respectively.

YAC Library Screening

A 4X chromosome 11 YAC library (Qin et al. 1993) was screened by PCR using microsatellite markers and the pooling scheme described in Qin et al. (1996). DNA pools for the CEPH-A library (Albertson et al. 1990) were obtained from Research Genetics and screened with primers for *D11S1310*. In some cases, small YAC contigs nucleated with an STS marker were expanded using an *Alu*–PCR hybridization strategy (Qin et al. 1996).

PAC Library Screening

PAC clones were identified in libraries RPCI-1, 3, 5, and 6, constructed as described (Ioannou et al. 1994), but in the pCYPAC2 or pPAC4 (RPCI-6) vectors. Pools of radiolabeled probes were hybridized to high-density filters each containing ~18,000 unique clones. Positive clones were grown in 96-well plates, transferred to filter replicates, and hybridized to individual probes as described (Ioannou et al. 1994). A variety of probes were used to detect clones, including PCR products generated from STSs, *Alu*–PCR products derived from YACs (Qin et al. 1996), and end fragments isolated from PACs (see below). All probes were labeled by random-priming (Feinberg and Vogelstein 1983) and hybridized as described (Church and Gilbert 1984).

YAC and PAC End Isolation

The ends of YAC inserts were isolated by the ligation-mediated PCR method of Kere et al. (1992). PAC insert ends were rescued by a modification of this method using vector primers immediately adjacent to the *Bam*HI cloning site in pCYPAC2 or pPAC4 (Cooper et al. 1997).

Clone Verification and Contig Assembly

After preparing individual YAC DNA in agarose by the lyticase/lithium dodecyl sulfate method (Anand et al. 1990), each clone was tested by PCR with the STS used to identify it. Overlap detected by hybridization of *Alu*–PCR products was confirmed by Southern analysis of *Alu*–PCR fingerprints. YACs were sized by pulsed-field gel electrophoresis using a CHEF–DRII apparatus (Bio-Rad) in 1% agarose gel (0.5× TBE) with a 10- to 50-sec switch time ramp (200 V, 29 hr), blotting to Gene Screen Plus (NEN), and hybridization with human Cot1 DNA (GIBCO BRL).

PAC DNA was prepared by an alkaline/SDS lysis procedure. PAC clones identified by *Alu*–PCR products from YACs were labeled by random priming and mapped back to YAC clones by Southern blotting. All other PAC clones were verified by Southern hybridization with single-copy plasmid probes and gel-purified STS-generated PCR products. Isolated end probes were used to confirm overlap between clones by Southern hybridization and to extend initial contigs by rescreening high-density PAC filters. PAC inserts were sized by *Not*I digestion of clone DNA and separation in CHEF gels as described above but with a switch time of 8 sec and running time of 22 hr.

YAC clones were mapped by FISH as part of a larger project (Qin et al. 1993, 1996). PAC clones were localized by FISH essentially as described (Sait et al. 1994) using between 100 and 200 ng of clone DNA. Contigs were assembled using the program SEGMAP (C. Magness, Y. Xu, and P. Green, unpubl.).

Large-Scale Sequencing

Large-insert bacterial clones were shotgun cloned into M13 phage and sequenced. The single-pass sequence traces from 1000 to 1500 clones per PAC were analyzed by Phred (P. Green and B. Ewing, University of Washington, Seattle) and assembled into contigs using Phrap (P. Green). Genomic DNA sequence was assessed for gene coding potential using the client program PowerBLAST (ftp://ncbi.nlm.nih.gov/pub/sim2/PowerBLAST/) and a network version of GRAIL (http://avalon.emp.ornl.gov/GRAIL-bin/EmptyGrailForm). The latter web page provided for the identification of CpG islands as defined by Gardiner-Garden and Frommer (1987).

Mutation Analysis of the *NEFA* Gene

Total RNA was isolated from lymphoblast cell cultures of affected and nonaffected individuals using the RNeasy minikit (Qiagen). Following treatment with RNase-free DNase (GIBCO BRL), first-strand cDNA synthesis was carried out using an oligo(dT) primer and Superscript reverse transcriptase (GIBCO BRL) as described by the manufacturer. PCR was then performed using eight oligonucleotides designed to amplify all of the *NEFA* cDNA (GenBank accession no. X76732) in four amplimers, each 400–500 bp in length. The primer sequences were F1, CGCCGACACCCGGCCAAGAAC; R1, CCAGTTCTTTGCTTAGCCTCCC; F2, CTCAAGCAAGTGATTGATGTGCTGG; R2, GCTTCCTGGGTGATTAACTTTAGG; F3, GGAACACTATGACAAGACTCGTCA; R3, ACTCCTCCAGAGTCACCAATCTG; F4, GAAAGGCTTAGAATGAGGGAACATG; and R4, GAAATAGATGTTGAGTTAACAGC. Amplifications were done in GeneAmp PCR buffer with 1.5 mM

$MgCl_2$ (F1–R1 and F4–R4) or in TNK50 (Kere et al. 1992) (F2–R2 and F3–R3) using a touchdown program with two cycles each at annealing temperatures ranging from 63°C to 57°C (1 min each), followed by 25 cycles at an annealing temperature of 56°C. Together, these four amplimers cover the entire *NEFA* cDNA except for 50 bp of the 5′ UTR and 106 bp of the 3′ UTR. The four PCR products were cloned into pCR-Script Cam (Strategene). The clones were sequenced using fluorescently tagged dideoxy chain terminators and an ABI 373A sequencer. The sequence of the *NEFA* cDNA from an individual with USH1C was compared with the wild-type sequence using the computer program GeneWorks (Oxford Molecular Group).

ACKNOWLEDGMENTS

We thank Linda Haley for the FISH localizations, Peter Mayers and Greg Kohler for assistance with SEGMAP and computer graphics, and Donna Ovak and LaMoyne Taplin for preparing this manuscript. This work was supported by grants (T.B.S.) from the Roswell Park Foundation and the National Institutes of Health (HG00333 and EY10514). Grant support for R.J.H.S. was from the National Institute on Deafness and Other Communication Disorders (NIDCD) DC02046.

The publication costs of this article were defrayed in part by payment of page charges. This article must therefore be hereby marked ''advertisement'' in accordance with 18 USC section 1734 solely to indicate this fact.

REFERENCES

Albertson, H.M., H. Abderrahim, H.M. Cann, J. Dausset, D. LePaslier, and D. Cohen. 1990. Construction and characterization of a yeast artificial chromosome library containing seven haploid human genome equivalents. *Proc. Natl. Acad. Sci.* 87: 4256–4260.

Anand, R., J.H. Riley, R. Butler, J.C. Smith, and A.F. Markham. 1990. A 3.5 genome equivalent multi access YAC library: Construction, characterization, screening and storage. *Nucleic Acids Res.* 18: 1951–1956.

Avraham, K.B., T. Hasson, K.P. Steel, D.M. Kingsley, L.B. Russell, M.S. Mooseker, N.G. Copeland, and N.A. Jenkins. 1995. The mouse *Snell's waltzer* deafness gene encodes an unconventional myosin required for structural integrity of inner ear hair cells. *Nature Genet.* 11: 369–375.

Ayyagari, R., A. Nestorowicz, Y. Li, S. Chandrasekharappa, C. Chinault, P. van Tuinen, R.J.H. Smith, J.F. Hejtmancik, and M.A. Permutt. 1996. Construction of a YAC contig encompassing the Usher syndrome type 1C and familial hyperinsulinism loci on chromosome 11p14-15.1. *Genome Res.* 6: 504–514.

Baldwin, C.T., C.F. Hoth, J.A. Amos, E.O. da-Silva, and A. Milunksy. 1992. A exonic mutation in the HuP2 paired domain gene causes Waardenburg's syndrome. *Nature* 355: 637–638.

Barnikol-Watanabe, S., N.A. Gross, H. Gotz, T. Henkel, A. Karabinos, H. Kratzin, H.U. Barnikol, and N. Hilschmann. 1994. Human protein NEFA, a novel DNA binding/EF-hand/leucine zipper protein. Molecular cloning and sequence analysis of the cDNA, isolation and characterization of the protein. *Biol. Chem. Hoppe-Seyler.* 375: 497–512.

Chaib, H., J. Kaplan, S. Gerber, C. Vincent, H. Ayadi, R. Slim, A. Munnich, J. Weissenbach, and C. Petit. 1997. A newly identified locus for Usher syndrome type 1, USH1E, maps to chromosome 21q21. *Hum. Mol. Genet.* 6: 27–31.

Chumakov, I.M., P. Rigault, I. LeGall, C. Bellanne-Chantelot, A. Billault, S. Guillou, P. Soularue, G. Guasconi, E. Pollier, I. Gros et al. 1995. A YAC contig map of the human genome. *Nature* 377: 175–299.

Chung, W.K., J. Goldberg-Berman, L. Power-Kehoe, and R.L. Leibel. 1996. Molecular mapping of the *tubby* (*tub*) mutation on mouse chromosome 7. *Genomics* 32: 210–217.

Church, G.M. and W. Gilbert. 1984. Genomic sequencing. *Proc. Natl. Acad. Sci.* 81: 1991–1995.

Cooper, P.R., N.J. Nowak, M.J. Higgins, S.A. Simpson, H. Stoehr, B.H. Weber, D.S. Gerhard, P.J. de Jong, and T.B. Shows. 1997. A sequence ready high resolution physical map of the Best's macular dystrophy gene region in 11q12-13. *Genomics* 41: 185–192.

Fantes, J.A., K. Oghene, S. Boyle, S. Danes, J.M. Fletcher, E.A. Bruford, K. Williamson, A. Seawright, A. Schedl, I. Hanson et al. 1995. A high-resolution integrated physical, cytogenetic, and genetic map of the human chromosome 11: Distal p13 to proximal p15.1. *Genomics* 25: 447–461.

Feinberg, A.P. and B. Vogelstein. 1983. A technique for radiolabelling DNA restriction endonuclease fragments to high specific activity. *Anal. Biochem.* 132: 6–13.

Gardiner-Garden, M. and M. Frommer. 1987. CpG islands in vertebrate genomes. *J. Mol. Biol.* 196: 261–282.

Gessler, M., G.H. Thomas, P. Couillin, C. Junien, B.C. McGillivray, M. Hayden, G. Jaschek, and G.A.P. Bruns. 1989. A deletion map of the WAGR region on chromosome 11. *Am. J. Hum. Genet.* 44: 486–495.

Green, E.D. and P. Green. 1991. Sequence-tagged site (STS) content mapping of human chromosomes: Theoretical considerations and early experiences. *PCR Methods & Applic.* 1: 77–90.

Grimberg, J., S. Nawoschik, L. Belluscio, R. McKee, A. Turck, and A. Eisenberg. 1989. A simple and efficient non-organic procedure for the isolation of genomic DNA from blood. *Nucleic Acids Res.* 17: 390.

Heckenlively, J.R., B. Chang, L.C. Erway, C. Peng, N.L. Hawes, G.S. Hageman, and T.H. Roderick. 1995. Mouse model for Usher Syndrome: linkage mapping suggests homology to Usher Type 1 reported at human chromosome 11p15. *Proc. Natl. Acad. Sci.* 92: 11100–11104.

Higgins, M.J., N.J. Smilinich, S. Sait, A. Koenig, J. Pongratz, M. Gessler, C.W. Richard III, M.R. James, J.P. Sanford, B.-W.

Kim et al. 1994. An ordered NotI fragment map of human chromosome band 11p15. *Genomics* 23: 211–222.

Inagaki, N., T. Gonoi, J.P. Clement, N. Namba, J. Inazawa, G. Gonzalez, L. Aguilar-Bryan, S. Seino, and J. Bryan. 1995. Reconstruction of I_{KATP}: An inward rectifier subunit plus the sulfonylurea receptor. *Science* 270: 1166–1170.

Ioannou, P.A., CT. Amemiya, J. Garnes, P.J. Kroisel, H. Shizuya, C. Chen, M.A. Batzer, and P.J. de Jong. 1994. A new bacteriophage P1-derived vector for the propagation of large human DNA fragments. *Nature Genet.* 6: 84–89.

James, M.R., C.W. Richard III, J.J. Schott, C. Yousry, K. Clark, J. Bell, J.D. Terwilliger, J. Hazan, C. Dubay, A. Vignal et al. 1994. A radiation hybrid map of 506 STS markers spanning human chromosome 11. *Nature Genet.* 8: 70–76.

Kaplan, J., S. Gerber, D. Bonneau, J.M. Rozet, O. Delrieu, M.L. Briard, H. Dollfus, I. Ghazi, J.L. Dufier, J. Frezal et al. 1992. A gene for Usher syndrome type I (USH1A) maps to chromosome 14q. *Genomics* 14: 979–987.

Keats, B.J.B., N. Nouri, M.Z. Pelias, P.L. Deininger, and M. Litt. 1994. Tightly linked flanking microsatellite markers for the Usher Syndrome Type 1 locus on the short arm of chromosome 11. *Am. J. Hum. Genet.* 54: 681–686.

Kelsell, D.P., J. Dunlop, H.P. Stevens, N.J. Lench, J.N. Liang, G. Parry, R.F. Mueller, and I.M. Leigh. 1997. Connexin 26 mutations in hereditary non-syndromic sensorineural deafness. *Nature* 387: 80–83.

Kere, J., R. Nagaraja, S. Mumm, A. Ciccodicola, M. D'Urso, and D. Schlessinger. 1992. Mapping human chromosomes by walking with sequence-tagged sites from end fragments of yeast artificial chromosome inserts. *Genomics* 14: 241–248.

Kimberling, W.J. and C. Moller. 1995. Clinical and molecular genetics of Usher syndrome. *J. Am. Acad. Audiol.* 6: 63–72.

Kimberling, W.J., M.D. Weston, C. Moller, S.L. Davenport, Y.Y. Shugart, I.A. Priluck, A. Martini, M. Milani, and R.J. Smith. 1990. Localization of Usher syndrome type II to chromosome 1q. *Genomics* 7: 245–249.

Kimberling, W.J., C.G. Möller, S. Davenport, I.A. Priluck, P.H. Beighton, J. Greenberg, W. Reardon, M.D. Weston, J.B. Kenyon, J.A. Grunkemeyer et al. 1992. Linkage of Usher Syndrome Type I Gene (USH1B) to the long arm of chromosome 11. *Genomics* 14: 988–994.

Kleyn, P.W., W. Fan, S.G. Kovats, J.J. Lee, J.C. Pulido, Y.Wu, L.R. Berkemeier, D.J. Misumi, L.M. Holmgren, O. Charlat et al. 1996. Identification and characterization of the mouse obesity gene *tubby:* A member of a novel gene family. *Cell* 85: 281–290.

Koa, F.T., C. Jones, and T.T Puck. 1976. Genetics of somatic mammalian cells: Genetic, immunologic and biochemical analysis with Chinese hamster cell hybrids containing selected human chromosomes. *Proc. Natl. Acad. Sci.* 73: 193–197.

Li, X., J. Luna, P.J. Lombroso, and U. Francke. 1995. Molecular cloning of the human homolog of a striatum-enriched phosphatase (STEP) gene and chromosomal mapping of the human and murine loci. *Genomics* 28: 442–449.

Liu, X.Z., J. Walsh, P. Mburu, J. Kendrickjones, M.J.T.V. Cope, K.P. Steel, and S.D.M. Brown. 1997. Mutations in the MYOSIN VIIA gene cause non-syndromic recessive deafness. *Nature Genet.* 16: 188–190.

Marietta, J., K.S. Walters, R. Burgess, L. Ni, K. Fukushima, K.C. Moore, J.F. Hejtmancik, and R.J.H. Smith. 1997. Usher syndrome type 1C: Clinical studies and fine mapping the disease locus. *Ann. Otol. Rhinol. Laryngol.* 106: 123–128.

Nestorowicz, A., B.A. Wilson, K.P. Schoor, H. Inoue, B. Glaser, H. Landau, C.A. Stanley, P.S. Thornton, J.P. Clement IV, J. Bryan et al. 1996. Mutation in the sulfonylurea receptor gene area associated with familial hyperinsulinism in Ashkenazi Jews. *Hum. Mol. Genet.* 5: 1813–1822.

Ohlemiller, K.K., R.M. Hughes, J. Mosinger-Ogilvie, J.D. Speck, D.H. Grosof, and M.S. Silverman. 1995. Cochlear and retinal degeneration in the *tubby* mouse. *NeuroReport* 6: 845–849.

Pieke-Dahl, S., W.J. Kimberling, M.B. Gorin, M.D. Weston, J.M. Furman, A. Pikus, and C. Moller. 1993. Genetic heterogeneity of Usher syndrome type II. *J. Med. Genet.* 30: 843–848.

Qin, S., J. Zhang, C. Isaacs, S. Nafaguchi, S.N.J. Sait, K. Abel, M. Higgins, N. Nowak, and T.B. Shows. 1993. A chromosome 11 YAC library. *Genomics* 16: 580–585.

Qin, S., N.J. Nowak, J. Zhang, S.N.J. Sait, P.G. Mayers, M.J. Higgins, Y.-J. Cheng, L. Li, D.J. Munroe, D.S. Gerhard et al. 1996. A high-resolution physical map of human chromosome 11. *Proc. Natl. Acad. Sci.* 93: 3149–3154.

Sait, S.N.J., N.J. Nowak, P. Singh-Kahlon, R. Weksberg, J. Squire, T.B. Shows, and M.J. Higgins. 1994. Localization of Beckwith-Wiedemann and rhabdoid tumor chromosome rearrangements to a defined interval in chromosome band 11p15.5. *Genes Chrom. Cancer* 11: 97–105.

Sankila, E.M., L. Pakarinen, H. Kaariainen, K. Aittomaki, S. Karjalainen, P. Sistonen, and A. de la Chapelle. 1995. Assignment of an Usher syndrome type III (USH3) gene to chromosome 3q. *Hum. Mol. Genet.* 4: 93–98.

Sellar, G.C., K. Oghene, S. Boyle, W.A. Bickmore, and A.S. Whitehead. 1994. Organization of the region encompassing the human serum amyloid A (SAA) gene family on chromosome 11p15.1. *Genomics* 23: 492–495.

Smith, R.J.H., E.C. Lee, W.J. Kimberling, S.P. Daiger, M.Z. Pelias, B.J.B. Keats, M. Jay, A. Bird, W. Reardon, M. Guest et al. 1992. Localization of two genes for Usher Syndrome Type I to chromosome 11. *Genomics* 14: 995–1002.

Smith, R.J.H., C. Berlin, J.F. Hejtmanci, B. Keats, W.J. Kimberling, R.A. Lewis, C.G. Moller, M.Z. Pelias, and L. Tranebjaerg. 1994. Clinical diagnosis of the Usher syndromes. *Am. J. Med. Genet.* 50: 32–38.

Strynadka, N.C.J. and M.N.G. James. 1989. Crystal structures of the helix-loop-helix calcium binding proteins. *Annu. Rev. Biochem.* 58: 951–998.

Tassabehji, M., A.R. Read, V.E. Newton, R. Harris, R. Balling, P. Gruss, and T. Strachan. 1992. Waardenburg's syndrome patients have mutations in the human homologue of the Pax-3 paired box gene. *Nature* 355: 635–636.

Thomas, P.M., G.J. Cote, N. Wohlil, B. Haddad, P.M. Mathews, W. Rabl, L. Aguilar-Bryan, R.F. Gagel, and J. Bryan. 1995. Mutations in the sulfonylurea receptor gene in familial persistent hyperinsulinemic hypoglycemia of infancy. *Science* 268: 426–429.

Wayne, S., V.M. der Kaloustian, M. Schloss, R. Polomeno, D.A. Scott, J.F. Hejtmancik, V.C. Sheffield, and R.J. Smith. 1996. Localization of the Usher syndrome type ID gene (USH1D) to chromosome 10. *Hum. Mol. Genet.* 5: 1689–1692.

Weil, D., S. Blanchard, J. Kaplan, P. Gullford, F. Gibson, J. Walsh, P. Mburu, A. Varela, J. Levilliers, M.D. Weston et al. 1995. Defective myosin VIIA gene responsible for Usher syndrome type 1B. *Nature* 374: 60–61.

Weil, D., P. Kussel, S. Blanchard, G. Levy, F. Leviacobas, M. Drira, H. Ayadi, and C. Petit. 1997. The autosomal recessive isolated deafness, DFNB2, and the Usher 1B syndrome are allelic defects of the myosin-VIIA gene. *Nature Genet.* 16: 191–193.

Weissenbach, J., G. Gyapay, C. Dib, A. Vignal, J. Morissette, P. Millasseau, G. Vaysseix, and M. Lathrop. 1992. A second-generation linkage map of the human genome. *Nature* 359: 794–801.

Whitehead Institute/MIT Center for Genome Research, Human Physical Mapping Project, Release 12, July 1997. http://www-genome.wi.mit.edu/cgi-bin/contig/phys_map.

Wolenski, J.S. 1995. Regulation of calmodulin-binding myosins. *Trends Cell Biol.* 5: 310–316.

Zhang, J. and T.L. Madden. 1997. PowerBLAST: A new network BLAST application for interactive or automated sequence analysis and annotation. *Genome Res.* 7: 649–656.

Received September 11, 1997; accepted in revised form December 15, 1997.